 MCB, vol.1, no.2, pp.101-111, 2004

# Forced Dissociation of the Strand Dimer Interface between C-Cadherin Ectodomains

**M.V. Bayas[1], K.Schulten[2] and D. Leckband[3]**

**Abstract:** The force-induced dissociation of the strand dimer interface in C-cadherin has been studied using steered molecular dynamics simulations. The dissociation occurred, without domain unraveling, after the extraction of the conserved trypthophans (Trp2) from their respective hydrophobic pockets. The simulations revealed two stable positions for the Trp2 side chain inside the pocket. The most internal stable position involved a hydrogen bond between the ring Nε of Trp2 and the backbone carbonyl of Glu90. In the second stable position, the aromatic ring is located at the pocket entrance. After extracting the two tryptophans from their pockets, the complex exists in an intermediate bound state that involves a close packing of the tryptophans with residues Asp1 and Asp27 from both domains. Dissociation occurred after this residue association was broken. Simulations carried out with a complex formed between W2A mutants showed that the mutant complex dissociates more easily than the wild type complex does. These results correlate closely with the role of the conserved tryptophans suggested previously by site directed mutagenesis.

**keyword:** C-cadherin, Cell Adhesion Molecules, Steered Molecular Dynamics.

## 1 Introduction

C-Cadherin, also called EP-Cadherin, is a representative classical cadherin expressed in the early embryo of the frog *Xenopus laevis* [Levi et al. (1991); Lee and Gumbiner (1995)]. It plays an important role in the transformation of a ball of undifferentiated cells into a well-organized embryo [Lee and Gumbiner (1995)]. As for all classical cadherins, C-cadherin comprises a highly conserved cytoplasmic domain, a single transmembrane segment and an extracellular segment containing a tandem of five cadherin-like domains [Takeichi (1990)]. The extracellular domains are numbered EC1 through EC5, starting from the N-terminal domain as shown in Fig. 1A. In the presence of $Ca^{++}$ these domains form a rigid structure necessary for adhesion [Nagar et al. (1996); Häussinger et al. (2002)].

The EC1 domain plays a central role in the adhesive activity of classical cadherins. It is thought to be responsible for the specificity of the interaction [Nose et al. (1990)]. Several studies demonstrated the importance of two elements of the EC1 domain in adhesion: namely, the conserved Trp2 and the hydrophobic pocket in the vicinity of the conserved HAV sequence [Blaschuk et al. (1990); Nose et al. (1990); Shapiro et al. (1995); Boggon et al. (2002); Häussinger et al. (2002)]. The recent X-ray structure of C-cadherin suggested that Trp2 is important for the *trans* association of classical cadherins [Boggon et al. (2002)]. According to this study the interacting cadherins form a strand dimer interface This interface involves an exchange of EC1 domain β-strands with the insertion of the conserved Trp2 side chain into the hydrophobic pocket in the opposite molecule (Fig. 1B). The exchanged β-strands form an anti-parallel β conformation involving hydrogen bonds between residues 1 to 3 of strand A and residues 27 to 25 of the partner B strand.

The evidence favoring the role of the *trans* strand dimer interface in adhesion is not completely conclusive. Site directed mutagenesis experiments demonstrated the importance of the Trp2 and the hydrophobic pocket for adhesive function [Tamura et al. (1998)]. However these experiments cannot discriminate between *trans* or *cis* associations. Moreover, electron microscopy studies showed that the mutation W2A abolishes *trans* but not *cis* interactions between chimeric E-cadherins [Pertz et al. (1999)]. To further complicate this scenario, recent ex-

[1] Center for Biophysics and Computational Biology, UIUC, Urbana, IL, U.S.A.
[2] Beckman Institute and Physics Department, Center for Biophysics and Computational Biology, UIUC, Urbana, IL, U.S.A.
[3] Chemical and Biomolecular Engineering, Center for Biophysics and Computational Biology, UIUC, Urbana, IL, U.S.A.

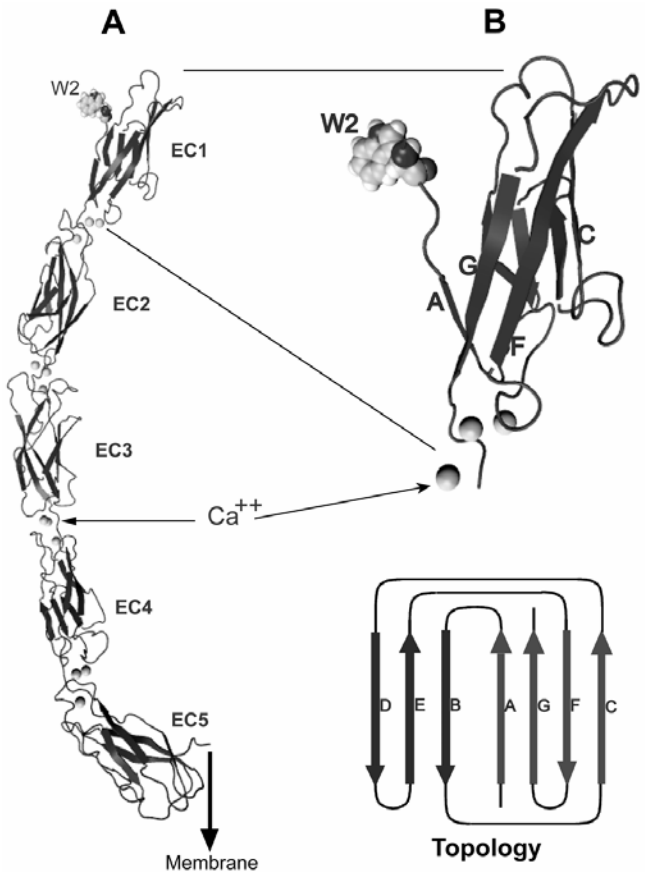


**Figure 1** : A) C-Cadherin ectodomain as modeled by Boggon et al. (2002). B) Cartoon representation of domain EC1 with the conserved Trp2 shown in VDW representation.

periments with desmosomal cadherins [He et al. (2003)] demonstrated the possibility that the Trp2-pocket association can participate in both *trans* and *cis* interactions.

Steered molecular dynamics (SMD) simulations [Isralewitz, Gao and Schulten. (2001)] offer an alternative way to test the ability of the *trans* strand dimer interface to resist force and thus form an adhesive bond. With this approach, an external force applied to the system of interest can induce ligand unbinding and/or conformational changes on time scales accessible to molecular dynamic simulations. Although the timescales are much shorter than in typical experiments, this approach has generated several results consistent with experimental observations [Marszalek et al. (1999); Isralewitz et al. (2001); Bayas et al. (2003); Craig et al. (2004); Park and Schulten. (2004)]. Consequently, SMD simulations can provide qualitative details concerning the stability of the *trans* dimer interface under force.

In this report, we used steered molecular dynamics (SMD) simulations to investigate the forced dissociation of the *trans* strand dimer interface between EC1 domains of C-Cadherin. Our results revealed the molecular details of the Trp2 interactions during complex dissociation and support the role of the Trp2 in stabilizing the *trans* association of the EC1 domains.

## 2 Methods

The steered molecular dynamic simulations were performed under both constant pulling velocity (cv-SMD) and constant force (cf-SMD) conditions, using the program NAMD [Kale et al. (1999)] and the CHARMM22 force field [MacKerell et al. (1998)]. Visualization, molecular graphics, and analysis of the simulations were performed using the program VMD [Humphrey et al. (1996)]. The crystal structure of the C-cadherin ectodomain deposited in the Brookhaven Protein Data Bank as entry 1L3W [Boggon et al. (2002)] was used as starting point. We used the structure of the EC1 domain (residues 1 to 104) to generate the strand dimer interface between two EC1 domains [Boggon et al. (2002)]. These domains will be referred as EC11 and EC12. The three calcium ions close to residues 102, 103 and 104 were also included. Figure 2A shows a representation of the final molecular complex. The z-axis was defined by the line joining the centers of mass of the backbone atoms of residues 102, 103 and 104 from both domains. The force was applied along the z-axis.

The complex was solvated in a box of explicit water molecules with dimensions 87.3 x 83.4 x 135.15 $Å^3$. The solvation was performed using the "solvate" feature of the VMD package [Humphrey et al. (1996)]. Ten $Cl^-$ ions and eight $Na^+$ ions were added to the system, keeping it neutral. The final system contained 93,539 atoms, 3,338 of which corresponded to the complex. The simulations were performed with a time step of 1 femtosecond, a uniform dielectric constant of 1, periodic boundary conditions, and a cutoff of nonbonded forces with a switching function starting at a distance of 10 Å and reaching zero at 14Å. Full electrostatic calculations were performed using the Particle Mesh Ewald method implemented in the NAMD package.

The energy of the system was initially minimized in two

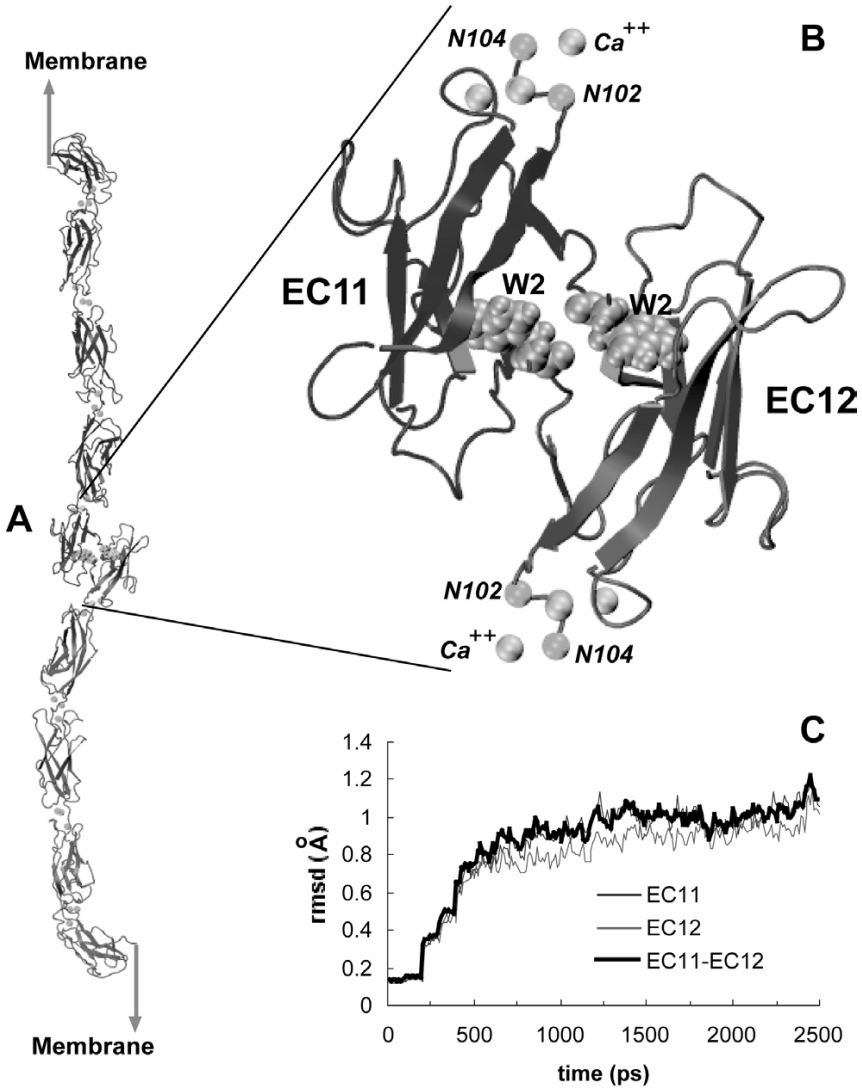


**Figure 2** : Construction of the system. A) Strand dimer interface between two C-Cadherin ectodomains based on the pdb entry 1L3W [Boggon et al. (2002)]. B) Detailed representation of the strand dimer interface containing only domains EC1. This is the molecular system used in the simulations. C) Evolution of the backbone rmsd as a function of time during the equilibration process.

stages. First, the coordinates of the complex were kept fixed for 10,000 steps of minimization. Then, allowing the free movement of the complex, except for the backbone atoms of residues 102, 103 and 104 in both EC1 domains, the system was minimized again for another 10,000 steps. The minimization was performed at 0 K followed by heating of the system to 298 K in 20,000 steps. During the heating, the atoms mentioned previously remained fixed.

Finally, the system was equilibrated at 298 K and 1 atm for 2.5ns. The temperature was controlled using Langevin dynamics, and the pressure was controlled with the Langevin piston pressure control. First, the system evolved for 0.5 ns under continuously decreasing restraints with the backbone atoms of residues 102, 103 and 104 from both EC1 domains still held fixed. After that, the system was allowed to evolve for 2 ns with the backbone atoms of EC11-102, 103 and 104 fixed, and the backbone atoms of EC12-102, 103 and 104 free to move only in the z direction. The backbone rmsd of the complex during the last 1 ns of equilibration was $1.197 \pm 0.045$ Å. Figure 2B shows the evo-

lution of the backbone rmsd during equilibration. The size of the water box at the end of the equilibration was 73.2x82.3x144.2 $Å^3$. The states at 1.5 and 2.5ns in the equilibration process were used as initial states for the SMD simulations. These included simulations of dissociation under a constant force of 300 pN. The purpose of the latter simulations was to study the system behavior when thermal fluctuations had an extensive opportunity to contribute to complex dissociation.

A separate set of simulations was performed using a system with the conserved tryptophans replaced with alanines (W2A mutant). This system was prepared as previously described for the wild type system. The only difference was that the system was equilibrated for only 1.5ns.

For simulations at constant pulling speed (cv-SMD) the backbone atoms of EC11-102, 103 and 104 were fixed whereas the backbone atoms of EC12-102, 103 and 104 were tagged as SMD atoms. This was done to prevent any distortion of the loop formed by these residues. The external force was applied along the z-axis and had the form:

$$F = k(vt - \Delta z). \quad (1)$$

Here $\Delta z$ is the z-displacement of the center of mass of the SMD atoms relative to its original position, v is the velocity of one end of a harmonic spring as if it were attached to the pulled atoms by the other end [Lu et al. (1998)], and k is the spring constant. The simulations were performed with a spring constant of 1 $k_BT/Å^2$ and pulling speeds of 1 and 0.1 Å/ps, which corresponds to loading rates of 70 and 7 pN/ps, respectively. For each velocity, the time evolution of the force (F) and the displacement $\Delta z$ were quantified. It is important to mention that $\Delta z$ is also the increment of the end-to-end distance of the complex in the direction of the applied force. In the following, $\Delta z$ will be referred as "extension".

In order to describe the behavior of the conserved tryptophans, the evolution in time of characteristic distances were evaluated. The distances between the center of mass of each tryptophan ring and the backbone carbon atom of residue 79 in the corresponding pocket describe the extraction of the rings from the pockets. Residue 79 is located in the innermost part of the pocket. The distances associated with the tryptophans from EC11 and EC12 will be called **d1** and **d2**, respectively. The relative distance **d12** between the centers of mass of the tryptophan rings describes the system evolution after the rings were extracted from the pockets.

## 3 Results

These simulations revealed three general features of the forced dissociation of the strand dimer interface. First, the dissociation occurred without unraveling the domains (see Fig. 3). Second, the complex dissociation occurred shortly after the side chains of the conserved tryptophans were extracted from their respective hydrophobic pockets. Third, there are two stable positions for the Trp2 side chain inside the pocket.

The cv-SMD simulations revealed the magnitude of the forces the complex can withstand on the nanosecond time scale. When the system was pulled at 1 Å/ps (70 pN/ps), the dissociation occurred in $\sim$0.1 ns and the maximum force was $\sim$2300 pN. The backbone rmsd of the domains after dissociation were $\sim$5 and $\sim$3 Å for EC11 and EC12 respectively. At 0.1 Å/ps (7 pN/ps) the complex dissociated in $\sim$0.5 ns and the maximum force was $\sim$800 pN. The corresponding backbone rmsd after dissociation for both EC11 and EC12 were $\sim$1.5 Å. None of these simulations revealed any substantial deformation of the EC1 domains during the pulling process. This is evident in figure 3, which shows snapshots from one of the simulations performed at the pulling speed of 1 Å/ps. Based on these results, we concluded that a force smaller than 500 pN, will dissociate the complex on nanosecond time scales, without significant domain deformation. Figures 4 and 5 show typical results of simulations carried out at the pulling rates of 1 and 0.1 Å/ps, respectively.

Figure 4A shows the force profile and the evolution of the extension with time when the complex was pulled at 1 Å/ps. At 21 ps (point 1) the slope in the force profile decreased because of a conformational change in EC11. This caused a jump in the corresponding rmsd (figure 4B). At 59 ps (point 2) the hydrogen bond between the ring Nε of Trp2 and the backbone carbonyl of Glu90 broke. This can be seen in figure 4C (curve a), which shows the evolution of the hydrogen bond length. Curve b (figure 4C) shows the distance associated with the salt bridge between the amino terminus of EC11 and residue 89 of EC12. Curve c (figure 4C) shows the distance associated with the salt bridge between residues EC11-D1 and EC12-N27. The complex dissociated after this contact was broken. The vertical dashed line in the plots indicates the final rupture. The conserved tryptophans always form close contacts during most of the simulation.

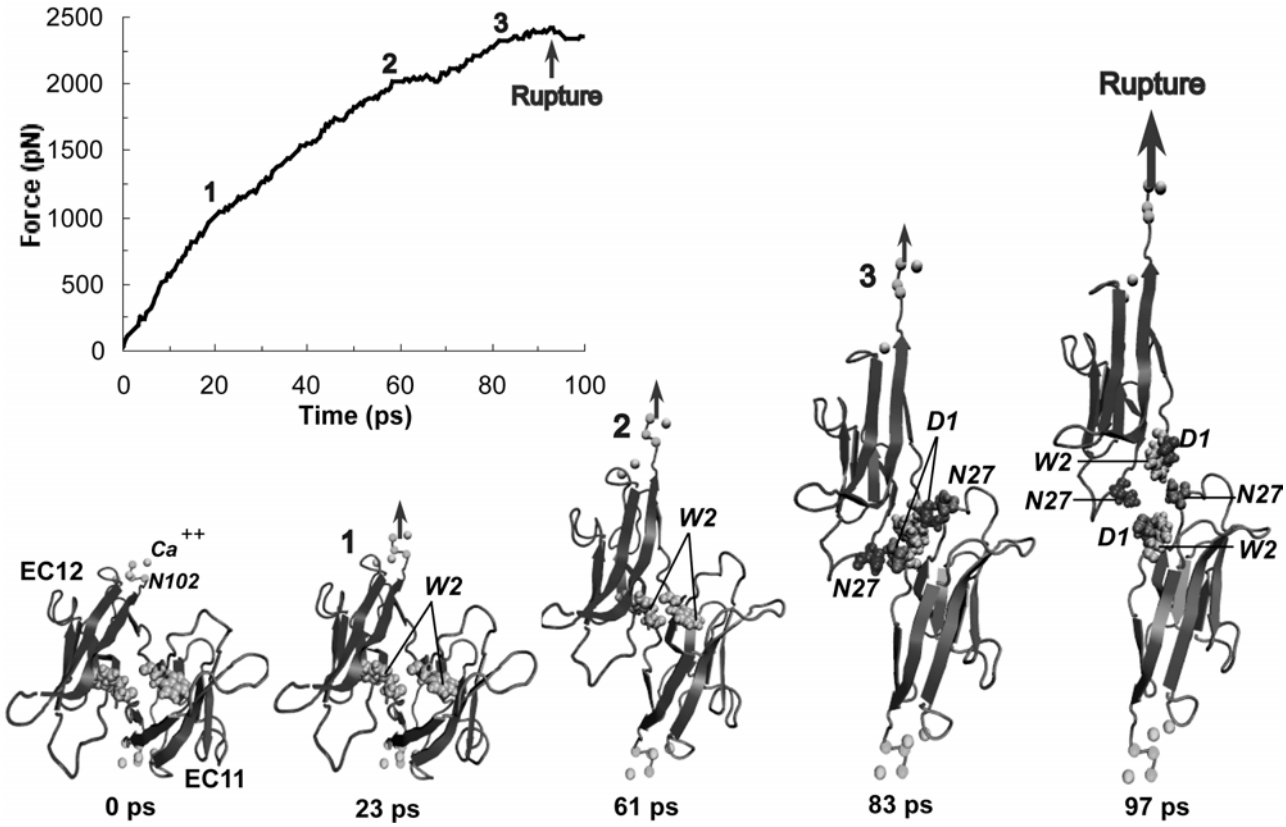


**Figure 3** : Snapshots of the complex during one of the simulations performed at 1 Å/ps. The inset shows the corresponding force-extension profile. The rupture process is mainly characterized by the extraction of the conserved tryptophan side chains from their pockets.

This can be seen in figure 4D, which shows the evolution in time of d12 and d1.

Figure 5A shows the force profile and the evolution of the extension with time when the complex was pulled at 0.1 Å/ps. At 58 ps (point 1) the slope in the force profile decreased because of a conformational change in EC11. The corresponding jump in the rmsd (figure 5B) was smaller than the one observed in the simulation at 1 Å/ps. At 280 ps (point 2) the hydrogen bond between the ring Nε of Trp2 and the backbone carbonyl of Glu90 broke. This can be appreciated in figure 5C (curve a), which shows the evolution of the hydrogen bond length. Figure 5C (curve b) shows the distance associated with the salt bridge between the amino terminus of domain EC11 and residue 89 of EC12. Figure 5D shows the evolution of **d12** and **d1**. At 280 ps (point 2) the aromatic ring of EC11-Trp2 started moving towards the entrance of the pocket where it remained for ∼100 ps. It finally pulled out of the pocket at 420 ps (point 3). After the two tryptophans were pulled from their pockets they packed in the tight conformation involving residues D1 and N27 from both domains (figure 3). This can be seen in the evolution of d12. The vertical dashed line in the plots indicates the rupture of this contact, and consequently the dissociation of the complex.

In general, the simulated trajectories show that, when pulled at constant velocity, the different contacts in the strand dimer interface break sequentially. First, the exchanged strands started to slowly separate. After this, because the domains were aligned with the pulling force, the conserved tryptophans started to take the tension. They remained completely inserted in their pockets until the hydrogen bond between the ring Nε of Trp2 and the backbone carbonyl of Glu90 broke (point 2 in figures 4 and 5). Then, Trp2 started to slowly move towards the entrance of the pocket. Before exiting the pocket, Trp2 remained in a stable position close to the entrance. The two Trp2 residues left their pockets to become trapped

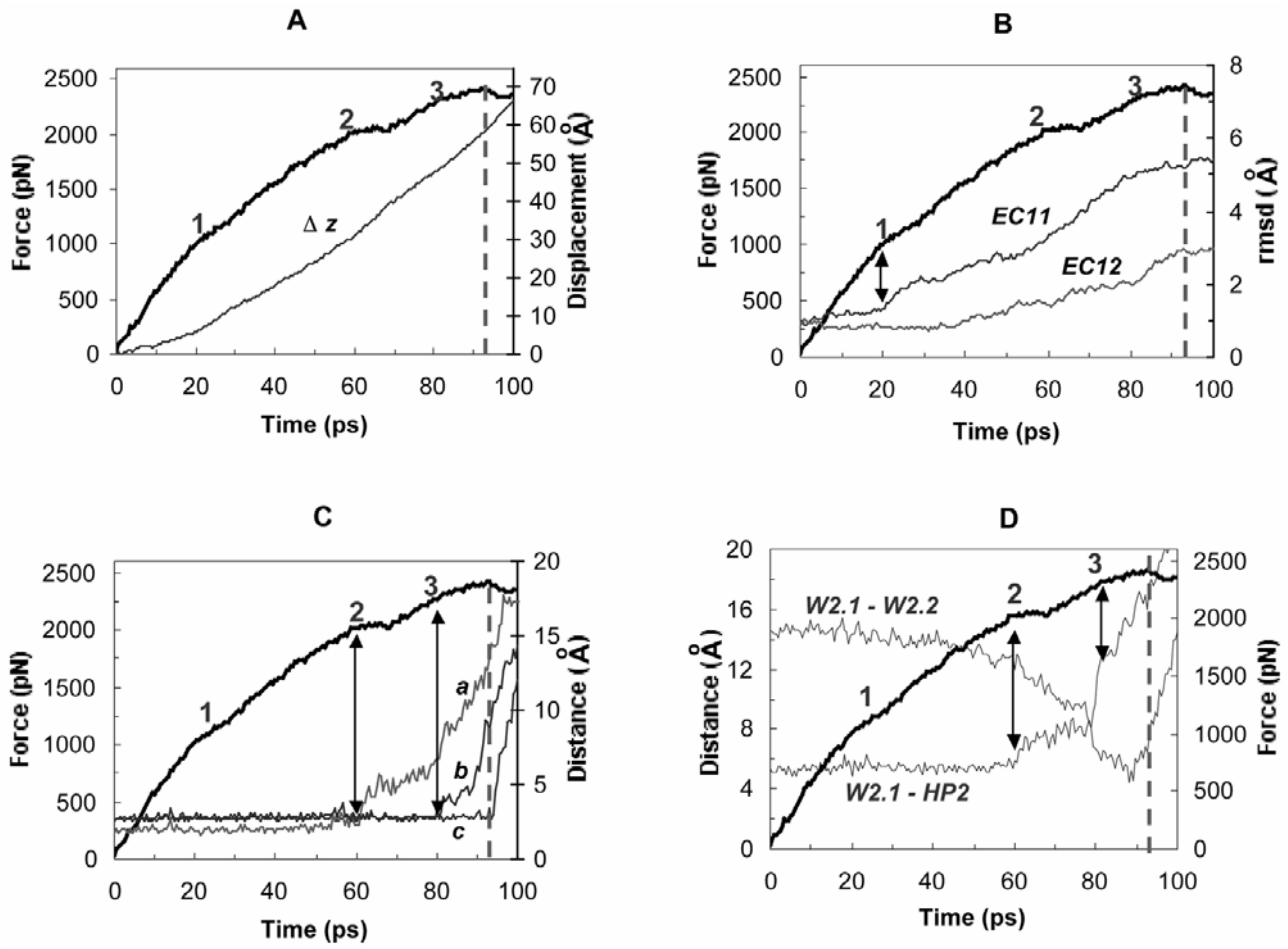


**Figure 4** : Results for one of the simulations performed at 1 Å/ps.

in an intermediate bound state involving the two tryptophans, EC11-D1, EC11-N27, EC12-D1 and EC12- N27 (see figure 3 at 83ps). The dissociation occurred when this association broke. The results of the cv-simulations are summarized in Table 1.

**Table 1** : Main results for the cv-SMD simulations.

| Pulling Speed (Å/ps) | Simulation | Equilibration time ( ns ) | Rupture force ( pN ) | Time at rupture ( ns ) |
|---|---|---|---|---|
| 1 | 1 | 1.5 | 2406 | 0.096 |
| | 2 | 1.5 | 2204 | 0.087 |
| | 3 | 2.5 | 2308 | 0094 |
| | 4 | 2.5 | 2145 | 0.086 |
| 0.1 | 1 | 1.5 | 825 | 0.526 |
| | 2 | 2.5 | 742 | 0.528 |

SMD simulations were also performed with a constant force of 300 pN. The force initially aligned the system extending the complex by $\sim$20Å. After that, contacts started breaking. The rupture events occurred in the same order as observed in the simulations at constant velocity. Each rupture caused a discrete increment in the complex extension. Complex dissociation occurred in $\sim$1.5 ns (Table. 2). The backbone rmsd of the domains, after dissociation, was $\sim$2 Å.

Figure 6 shows the results of one of the cf-simulations. Figure 6A shows the evolution of the complex extension for both the wild type complex and the W2A mutants. It can be appreciated that the dissociation of the complex involving W2A mutants occurred more rapidly. Figures 6B and 6C show the evolution of d1 and d2, respectively. There are two stable positions of the aromatic rings inside the pocket with d1 (d2) equal to $\sim$5 and $\sim$8 Å, respectively. Figure 6D shows the distance between

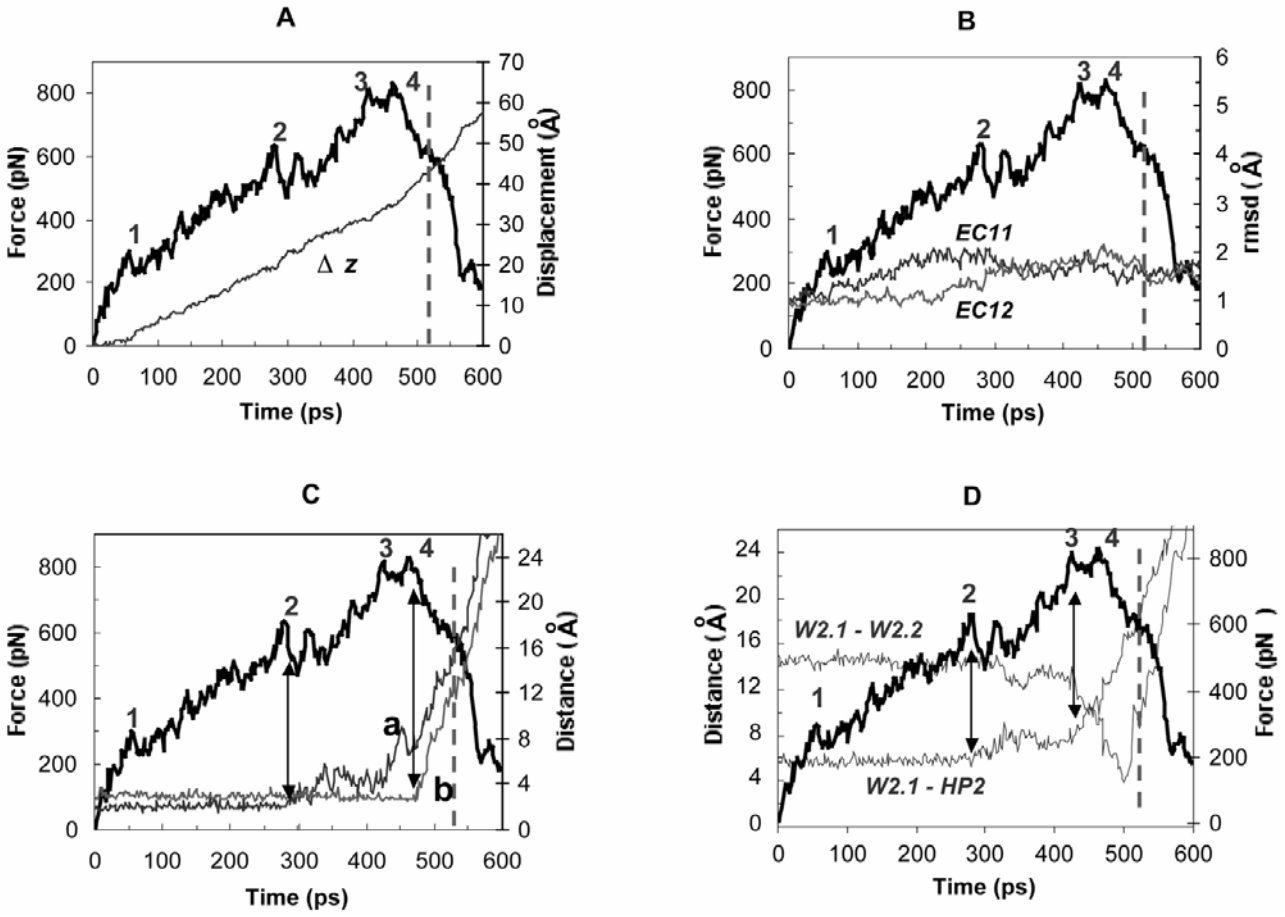


**Figure 5** : Results for one of the simulations performed at 0.1 Å/ps.

**Table 2** : Rupture times for the cf-simulations

| Simulation | Equilibration Time (ns) | Time at rupture (ns) |
|---|---|---|
| 1 | 1.5 | 1.49 |
| 2 | 2.5 | 1.77 |
| 3 | 2.5 | 1.34 |

the center of mass of the Trp2 aromatic rings from both domains (d12). This distance decreased as the aromatic rings were extracted from the pockets. This is due to the close packing of the rings mentioned previously. As in the cv-simulations, dissociation occurred after the intermediate bound state involving the two tryptophans broke.

The simulations at constant force clearly showed the several intermediate bound states associated with the different stable positions of the conserved tryptophans. The innermost stable position involving the tryptophan side chains inside their pockets corresponded to d1 (d2) equal to $\sim$5 Å. In this position the hydrogen bond between the ring N$\varepsilon$ of Trp2 and the backbone carbonyl of Glu90 remained unbroken. In the second stable position the tryptophan side chains were located at the edge of the pocket. This corresponded to a value of d1 (d2) equal to $\sim$8 Å. The complex extension was $\sim$30 Å when the two tryptophans were extracted from their pockets. As in the cv-SMD simulations, after leaving the pockets, the two tryptophans became trapped in another intermediate bound state involving residues D11 and N27 of the two domains. Complex dissociation occurred after the contacts, in this last intermediate state, broke. The results from the cf-simulations are summarized in Table 2.

The simulations with the W2A mutants clearly showed a weaker bond. When pulled at constant velocity the forces

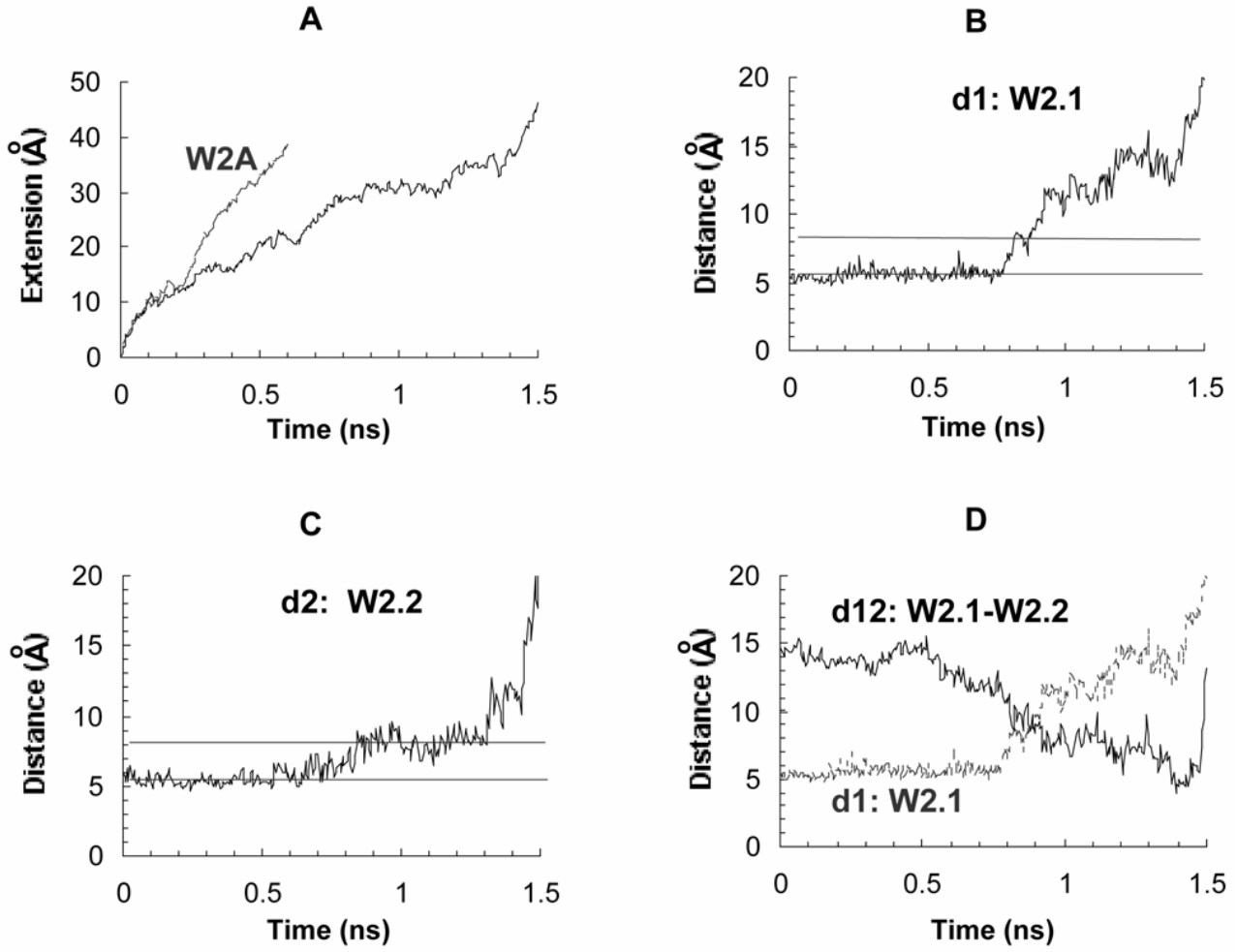


**Figure 6** : Evolution of representative distances when the system was pulled with a constant force of 300 pN.

necessary for dissociation were smaller than the ones for the wild type complex, namely: ∼90% and ∼75% of the values obtained at 1 Å/ps and 0.1 Å/ps, respectively. On the other hand, when the complex was pulled with a constant force of 300 pN, the time necessary for rupture was ∼40% of the time required to dissociate the wild type complex (see Fig. 6A). The absence of the hydrogen bond between the ring Nε of Trp2 and the backbone carbonyl of Glu90 and the small size of the alanine side chains eliminated the intermediate states observed for the wild type complex and, therefore, made the dissociation easier. Table 3 summarizes the main results of all simulations.

**Table 3** : Dissociation forces and times for all the simulations. Average values are shown.

| Simulation | Dissociation force (pN) | | Time for dissociation (ns) | |
|---|---|---|---|---|
| | W2A | Wild type | W2A | Wild type |
| 1 Å/ps | 1982 | 2266 | 0.088 | 0.091 |
| 0.1 Å/ps | 585 | 784 | 0.46 | 0.53 |
| 300 pN | -- | -- | 0.62 | 1.53 |

## 4 DISCUSSION

The SMD simulations in the present study showed two important features of the mechanical response to force of the *trans* strand dimer interface between the EC1 domains of C-cadherin. First, domain unfolding does not occur during dissociation of the adhesive complex on the nanosecond time scale. Second, the extraction of the conserved tryptophan side chains from their hydrophobic pockets is the central part of the dissociation process.

At constant pulling speed the bond ruptured at forces lower than the ones necessary to unravel the domains. A similar study with an adhesive complex involving Immunoglobulin (Ig) domains showed that partial unfolding was coupled to detachment at a loading rate of 70 pN/ps (1 Å/ps) [Bayas et al. (2003)]. The force for unfolding of the Ig domains was $\sim$2600 pN. Given the similarity between the Cadherin and Ig topologies, this value is a good reference to anticipate the involvement of unfolding during the detachment of the *trans* strand dimer. In the present study the *trans* strand dimer dissociated without unfolding at $\sim$2300 pN when pulled at 70 pN/ps. The absence of unfolding during dissociation was corroborated using the cf-SMD simulations. In these simulations, the system was pulled with a force lower than needed to significantly distort the domains in the cv-SMD simulations. These results suggest that domain unfolding is not coupled to the adhesive function of cadherins.

The importance of the conserved tryptophans for the stability of the *trans* strand dimer interface can be appreciated by looking at the different interactions they participate in. As the tryptophans were pulled out of the hydrophobic pockets, new contacts appeared and the complex resisted dissociation. This, in turn, determined the forces and times required for complex dissociation. These findings were corroborated by simulations with W2A mutants, which clearly exhibited a weaker bond. Particularly, when the W2A mutant complex was pulled with a constant force of 300 pN, the time necessary for dissociation was less than half the time required for the wild type complex. This shows that the substitution of the conserved tryptophans substantially decreased the complex energy.

Considering the fact that the direction of the applied forces in the simulations is the same as on the cell surface, these results show the Trp2-pocket association can resist an applied force and stabilizes the adhesive interface. However, this does not exclude the possibility of the participation of this interface in *cis* interactions. We will address this possibility in future studies.

The values of the forces and displacements necessary for bond rupture, obtained with the simulations cannot be compared directly with experiments. However, a qualitative extrapolation of the rupture process is justified. It has been demonstrated that, despite the fact that the time scales of MD simulations are several orders of magnitude smaller than those of typical experiments, the SMD results and experiments are not totally disconnected [Evans and Ritchie (1997); Isralewitz et al. (2001); Craig et al. (2004); Park and Schulten. (2004)]. The present study suggests a rationale for the importance for adhesion of the Trp2-hydrophobic pocket association in agreement with some experimental results.

In summary, the SMD simulations presented in this paper provided molecular level insight into the dissociation mechanism of the *trans* strand dimer interface between C-cadherin EC1 ectodomains under force. The tensile strength is determined by the molecular contacts involved in the Trp2-Pocket association. This is consistent with the result of site directed mutagenesis experiments. Importantly, the different stable conformations the system can adopt during the pulling process suggest a possible mechanism for the selectivity among cadherins. The selectivity might originate in differences between the set of stable conformations in a particular interaction. However, more studies are necessary to test this hypothesis.

**Acknowledgement:** This work was supported by grants from the National Institutes of Health: NIH PHS 2 P41 RR05969 (KS) and 1RO1 GM51338-10 (DEL). The authors also wish to acknowledge computer time provided at the NSF centers by the grant NRAC MCA93S028. Figures in this article were produced with the program VMD [Humphrey et al. (1996)]

## References

**Bayas, M. V.; Schulten, K.; Leckband, D.** (2003): Forced detachment of the CD2-CD58 complex. *Biophys. J.* vol. 84, pp. 2223-2233.

**Blaschuk, O. W.; Sullivan, R.; David, S.; Pouliot, Y.** (1990): Identification of a cadherin cell adhesion recognition sequence. *Dev. Biol*, vol. 139, pp. 227-229.

**Boggon, T. J.; Murray, J.; Chappuis-Flament, S.;**

**Wong, E.; Gumbiner, B. M.; Shapiro, L.** (2002): C-Cadherin Ectodomain Structure and Implications for Cell Adhesion Mechanisms. *Science*, vol. 296, pp. 1308-1313.

**Chappuis-Flament, S.; Wong, E.; Hicks, L. D.; Kay, C. M.; Gumbiner, B. M.** (2001): Multiple cadherins extracellular repeats mediate homophilic binding and adhesion. *J. Cell. Biol*, vol. 154, pp. 231-243.

**Craig, D.; Gao, M.; Schulten, K.; Vogel, V.** (2004): Tuning the mechanical stability of fibronectin type III modules through sequence variation. *Structure*, vol. 12, pp. 21-30.

**Evans, E.; Ritchie, K.** (1997): Dynamic Strength of Molecular Adhesion Bonds. *Biophys. J*, vol. 72, pp.1541-1555.

**Gumbiner, B. M.** (1996): Cell Adhesion: The Molecular Basis of Tissue Architecture and Morphogenesis. *Cell*, vol. 84, pp. 345-357.

**Haussinger, D.; Ahrens, T.; Sass, H-J.; Pertz, O.; Engel, J.; Grzesiek, S.** (2002): Calcium-dependent Homoassociation of E-cadherin by NMR Spectroscopy: Changes in Mobility, Conformation and Mapping of Contact Regions. *J. Mol. Biol*, vol. 324, pp. 823-839.

**He, W.; Cowin, P.; Stokes, D. L.** (2003): Untangling Desmosomal Knots with Electron Tomography. *Science*, vol. 302, pp.109-113.

**Humphrey, W.; Dalke, A.; Schulten, K.** (1996): VMD visual molecular dynamics. *J. Mol. Graphics*, vol. 14, pp. 33-38.

**Isralewitz, B.; Gao, M.; Schulten, K.** (2001): Steered molecular dynamics and mechanical functions of proteins. *Curr. Opin. Struct. Biol*, vol. 11, pp.224-230.

**Isralewitz, B.; Baudry, J.; Gullingsrud, J.; Kosztin, D.; Schulten, K.** (2001): Steered molecular dynamics investigations of protein function. *J. Mol. Graph. Mod*, vol. 19, pp.13-25.

**Izrailev, S.; Stepaniants, S.; Balsera, M.; Oono, Y.; Schulten, K.** (1997): Molecular Dynamics Study of Unbinding of the Aviding-Biotin Complex. *Biophys. J*, vol. 72, pp.1568-1581.

**Kale, L. V.; Skeel, R. D.; Bhandarkar, M.; Brunner, R.; Gursey, A.; Krawetz, N.; Philips, J.; Shinazaki, A.; Varadarajan, K.; Schulten, K.** (1999): NAMD2: Greater scalability for parallel molecular dynamics. *J. Comp. Phys*, vol. 151, pp. 283-312.

**Lee, C-H.; Gumbiner, B.** (1995): Disruption of Gastrulation Movements in *Xenopus* by a Dominant-Negative Mutant for C-Cadherin. *Dev. Biol*, vol. 171, pp.363-373.

**Levi, G.; Ginsberg, D.; Girault, J.; Sabanay, I.; Thiery, J. P.; Geiger, B.** (1991): EP-Cadherin in muscles and epithelia of *Xenopus laevis* embryos. *Development*, vol. 113, pp. 1335-1344.

**Lu, H.; Isralewitz, B.; Krammer, A.; Vogel, V.; Schulten, K.** (1998): Unfolding of Titin Immunoglobulin Domains by Steered Molecular Dynamics Simulation. *Biophys. J*, vol. 75, pp. 662-671.

**MacKerell, A. D.; Bashford, D.; Bellot, M.; Dunbrack, R. L Jr.; Evansec, J.; Field, M. J.; Fisher, S.; Gao, J.; Guo, H.; Ha, S.; Joseph, D.; Kuchnir, L.; Kuczera, K.; Lau, F. T. K.; Mattos, C.; Michnick, S.; Ngo, T.; Nguyen, D. T.; Prodhom, B.; Reiher, I. W. E.; Roux, B.; Schlenkrich, M.; Smith, J.; Stote, R.; Straub, J.; Watanabe, M.; Wiorkiewicz-Kuczera, J.; Yin, D.; Karplus, M.** (1998): All-hydrogen empirical potential for molecular modeling and dynamics studies of protein using the CHARMM22 force field. *J. Phys. Chem. B*, vol. 102, pp. 3586-3616.

**Marszalek, P. E.; Lu, H.; Li, HB.; Carrion-Vazquez, M.; Oberhauser, A. F.; Schulten, K.; Fernandez, J. M.** (1999): Mechanical unfolding intermediates in titin modules. *Nature*, vol. 402, pp. 100-103.

**Nagar, B.; Overduin, M.; Ikura, M.; Rini, J. M.** (1996): Structural basis of calcium-induced E-cadherin rigidification and dimerization. *Nature*, vol. 380, pp. 360-364.

**Niessen, C. M.; Gumbiner, B. M.** (2002): Cadherin-mediated cell sorting not determined by binding or adhesion specificity. *J. Cell. Biol*, vol. 156, pp. 389-399.

**Nose, A.; Tsuji, K.; Takeichi, M.** (1990): Localization of specificity determining sites in cadherin cell adhesion molecules. *Cell*, vol. 61, pp. 147-155.

**Park, S.; Schulten, K.** (2004): Calculating potentials of mean force from steered molecular dynamics simulations. *Journal of Chemical Physics*, vol. 120, pp. 5946-5961.

**Pertz, O.; Bozic, D.; Koch, A. W.; Fauser, C.; Brancaccio, A.; Engel, J.** (1999): A new crystal, $Ca^{2+}$ dependence and mutational analysis reveal molecular details of E-cadherin homoassociation. *EMBO J*, vol. 18, pp. 1738-1747.

**Shapiro, L.; Fannon, A. M.; Kwong, P. D.; Thompson, A.; Lehmann, M. S.; Grubel, G.; Legrand, J-F.; Als-Nielsen, J.; Colman, D. R.; Hendrickson, W. A.** (1995): Structural basis of cell-cell adhesion by cadherins. *Nature*, vol. 374, pp. 327-337.

**Takeichi, M.** (1990): Cadherins: A molecular family important in selective cell-cell adhesion. *Annu. Rev. Biochem*, vol. 59, pp. 237-252.

**Tamura, K.; Shan, W-S.; Hendrickson, W. A.; Colman, D. R.; Shapiro, L.** (1998): Structure-Function Analysis of Cell Adhesion by Neural (N-) Cadherin. *Neuron*, vol. 20, pp. 1153-1163.